ELSEVIER

Cement & Concrete Composites 24 (2002) 339–346

Cement & Concrete Composites

www.elsevier.com/locate/cemconcomp

Study of thaumasite and ettringite phases formed in sulfate/blast furnace slag slurries using XRD full pattern fitting

S.J. Barnett [a,1], M.A. Halliwell [b], N.J. Crammond [b], C.D. Adam [a,*], A.R.W. Jackson [a]

[a] School of Sciences, Staffordshire University, College Road, Stoke-on-Trent ST4 2DE, UK
[b] Building Research Establishment Limited, Garston, Watford WD2 7JR, UK

Abstract

The thaumasite form of sulfate attack (TSA) has been investigated using a method known to accelerate the formation of the sulfate minerals thaumasite, ettringite and gypsum. Mixes containing different cements and aggregates in magnesium sulfate solution were prepared at different water:solid ratios. The work concentrated, in particular, on the role of blast furnace slag as a cementitious material in preventing the formation of thaumasite. The formation of sulfate minerals in the mixes was followed for a period of two years by X-ray powder diffraction. Full pattern fitting, a computer-based XRD data analysis technique, was used to identify the nature of the thaumasite/ettringite solid solutions produced. Thaumasite was formed only in mixes containing carbonate-bearing aggregates at higher water:solid ratios. In most of the mixtures containing blast furnace slag cement (70% blast furnace slag cement, 30% Portland cement), an ettringite-based solid solution was the main sulfate-bearing phase produced. Only one of the mixes containing blast furnace slag cement was found to produce thaumasite. Some samples, containing only blast furnace slag as the cementitious component, produced gypsum and no thaumasite/ettringite. The variation in the exact nature of thaumasite/ettringite produced with different aggregates, cements and water:solid ratios is discussed.

Keywords: Thaumasite formation; Sulfate attack; XRD

1. Introduction

Thaumasite ($Ca_3SiSO_4CO_3(OH)_6 \cdot 12H_2O$) and ettringite ($Ca_6Al_2(SO_4)_3(OH)_{12} \cdot 26H_2O$) are both naturally occurring minerals [1,2] which are also formed during the attack on concrete by sulfate solutions [3–5]. The occurrence of the thaumasite form of sulfate attack (TSA) relies on the co-existence of several conditions, namely:- wet, cold, available supply of sulfate and carbonate ions, presence of reactive silica and alumina [3]. The occurrence of TSA has been considered to be relatively rare. Recently however, several cases have come to light in the UK, resulting in the convening of the Thaumasite Expert Group in April 1998 [6]. The formation of thaumasite consumes the C–S–H in a cement paste. This reduces the binding ability of the cement leading to a loss of strength and degradation of the concrete into an incohesive mass.

Thaumasite has a structure based on columns of composition $[Ca_3Si(OH)_6 \cdot 12H_2O]^{4+}$ with the sulfate and carbonate anions lying in channels between the columns [7]. It is hexagonal (space group $P6_3$) with $a = 11.054$ Å, $c = 10.410$ Å [8]. Ettringite has a similar structure with Si replaced by Al in the columns and $2SO_4^{2-}$ plus $2CO_3^{2-}$ replaced by $3SO_4^{2-}$ plus $2H_2O$ in the channels [9]. Ettringite is trigonal (space group P31c) with $a = 11.234$ Å, $c = 21.501$ Å [8]. The doubling of the c-dimension in ettringite is a result of the ordering of the anions in the channels of the structure.

The crystal structures of thaumasite and ettringite are sufficiently similar for solid solutions to occur [7,10,11], despite their different space groups. The identification of solid solution effects is complicated by the existence of other solid solutions formed within the ettringite structure [10–14], the solid solution between ettringite ($Ca_6Al_2(SO_4)_3(OH)_{12} \cdot 26H_2O$) and carbonate ettringite($Ca_6Al_2(CO_3)_3(OH)_{12} \cdot 26H_2O$) is likely to be the most significant of these [10,12]. There are several occurrences of solid solutions both in nature [15] and in

* Corresponding author. Present address: Department of Physics, School of Chemistry and Physics, Keele University, Keele, Staffordshire ST5 5BG, UK.
E-mail address: c.d.adam@keele.ac.uk (C.D. Adam).
[1] Present address: Department of Chemistry, University of Aberdeen, Meston Walk, Aberdeen AB24 3UE, UK.

0958-9465/02/$ - see front matter
PII: S0958-9465(01)00085-3

concrete subjected to sulfate attack [3,6]. The solid solution effects can be observed in X-ray powder diffraction patterns. The changes in intensity are minimal and in particular the extra reflections allowed by ettringite's lower symmetry are very weak and cannot be used to distinguish between an ettringite structure and a thaumasite structure [10,11]. However, there are significant changes in unit cell dimensions. With the aid of computer-based X-ray powder diffraction data analysis techniques, such as full pattern fitting and Rietveld refinement [16], it is possible to measure qualitatively the degree of solid solution present [10,11].

Full pattern fitting is a least squares minimisation technique, in which a refinable model is used to produce a calculated powder pattern which is then fitted to experimental data [16]. The technique is used to obtain accurate unit cell dimensions (±0.05%) and intensity measurements. The calculated data is produced from a model which includes the Miller indices of reflections present in the diffraction pattern, approximate unit cell dimensions, instrumental and sample dependent effects. The model is adjusted in an iterative procedure until a good fit of observed and calculated data is achieved. Relative intensities, unit cell parameters, 2θ corrections and peak profile coefficients are refined so as to produce the best fit to the experimental data. An early use of this technique, in which real Portland cement systems were quantified by fitting to standard patterns for the phases present, was made by Gutteridge [17]. The technique has also been shown to be valuable in the characterisation of thaumasite [18].

In the work presented here, the full pattern fitting technique has been applied to the analysis of thaumasite, ettringite and their solid solutions in samples previously prepared and examined by the Building Research Establishment (BRE). The examination of these samples at BRE had formed part of a larger study initiated in 1994 by the Department of the Environment, Transport and the Regions (DETR) and the Cementitious Slag Makers Association (CSMA). The samples comprised a series of slurries containing cementitious material, magnesium sulfate and ground limestone. As the aim of the BRE work was to investigate whether the use of ground granulated blast furnace slag (ggbfs) cement could be beneficial in avoiding the onset of TSA, the majority of the cementitious material present in the slurries contained ggbfs. The slurries were examined periodically using XRD and the results have been published in a BRE specialist Report [19]. In order to improve the accuracy of the BRE results and maximise the amount of information they could provide, the XRD raw data were also examined by Staffordshire University using the full pattern fitting technique [20] and it is these more detailed results which are described and discussed in this paper.

2. Experimental

Slurries of various different cements and aggregates in magnesium sulfate solutions were prepared in a procedure known to accelerate the formation of the sulfate minerals thaumasite, ettringite and gypsum [19]. The cements used were:

(i) Ordinary Portland Cement (OPC);
(ii) 70% slag 1 + 30% OPC;
(iii) 70% slag 2 + 30% OPC;
(iv) BRECEM (50% calcium aluminate cement + 50% ggbfs).

Table 1 gives the chemical analysis of these cements. The aggregates used were:

(i) Carboniferous limestone (CL) – mainly calcite with minor amounts of dolomite and trace amounts of quartz;
(ii) magnesian limestone (ML) – mainly dolomite with trace amounts of quartz;
(iii) flint – pure quartz.

The aggregates used were crushed to pass through a 150 μm sieve. The dry ingredients were dispersed in magnesium sulfate solution (containing 4.2 g/l SO_4^{2-}) at a high water:solid ratio. The slurries were aged at 5 °C, while being constantly agitated. 18 series were prepared. Within each series, the amount of solution was kept constant at 100 ml while the ratio of solid material was increased in order to vary the amount of sulfate avail-

Table 1
Chemical compositions of cements used

Chemical analysis	OPC	Slag 1	Slag 2
SiO_2	20.8	34.8	32.1
Al_2O_3	4.51	11.8	16.93
Fe_2O_3	2.86	1	0.75
CaO	64.1	41.4	35.8
MgO	1.22	8.3	10.5
K_2O	0.56	0.33	0.46
Na_2O	0.15	0.28	0.36
TiO_2	0.49		0.97
P_2O_5	0.07		
Mn_2O_3	0.09		0.55
BaO	0.01		0.16
SrO	0.06		0.07
SO_3	3.00		2.15
LOI	1.10		
Free lime	3.26		
C_4AF	8.8		
C_3A	7.2		
C_3S	48.6		
C_2S	23.7		

able. A detailed description of the mix compositions is given in Table 2.

The mineralogical changes which occurred in these mixtures were followed for two years by XRD at ages 1, 2, 3, 4, 5, 8, 12, 18 and 24 months. At the test dates, a small amount of material (approximately 0.5 cm^3) was drawn from the slurries using a pipette and allowed to dry naturally for 12 h. The dry residue was finely ground to pass through a 53 μm sieve and the powder was placed on a single crystal silicon slice for analysis. XRD patterns were collected on a fully automated Siemens D500 diffractometer operating at 40 kV and 30 mA using CuKα radiation. Data was collected between 5° and 50° 2θ using a step-size of 0.05° and a count time of 4 s per step.

The BESTFIT full pattern fitting program developed by Adam [20] was then used to obtain accurate unit cell dimensions for the thaumasite and/or ettringite-type phases present in the slurries. The error in the cell parameters is estimated to be ±0.005 Å for the *a*-axis and ±0.01 Å for the *c*-axis. All other phases present in the slurries were included in the fitting procedure, with the intensity and peak profile parameters of each reflection being refined independently and simultaneously.

Table 2
Composition of mixes studied

Series	Mix no.	Mix code	Cement component	Aggregate
OC	1	OC2	1 g OPC	1 g CL
	2	OC4	2 g OPC	2 g CL
	3	OC8	4 g OPC	4 g CL
OD	4	OD2	1 g OPC	1 g ML
	5	OD4	2 g OPC	2 g ML
	6	OD8	4 g OPC	4 g ML
OT	7	OT2	1 g OPC	1 g flint
	8	OT4	2 g OPC	2 g flint
	9	OT8	4 g OPC	4 g flint
OSC	10	OSC2	1 g OPC/slag1	1 g CL
	11	OSC4	2 g OPC/slag1	2 g CL
	12	OSC8	4 g OPC/slag1	4 g CL
OSD	13	OSD2	1 g OPC/slag1	1 g ML
	14	OSD4	2 g OPC/slag1	2 g ML
	15	OSD8	4 g OPC/slag1	4 g ML
OST	16	OST2	1 g OPC/slag1	1 g flint
	17	OST4	2 g OPC/slag1	2 g flint
	18	OST8	4 g OPC/slag1	4 g flint
OS2C	19	OS2C2	1 g OPC/slag2	1 g CL
	20	OS2C4	2 g OPC/slag2	2 g CL
	21	OS2C8	4 g OPC/slag2	4 g CL
OS2D	22	OS2D2	1 g OPC/slag2	1 g ML
	23	OS2D4	2 g OPC/slag2	2 g ML
	24	OS2D8	4 g OPC/slag2	4 g ML
OS2T	25	OS2T2	1 g OPC/slag2	1 g flint
	26	OS2T4	2 g OPC/slag2	2 g flint
	27	OS2T8	4 g OPC/slag2	4 g flint
SC	28	SC2	1 g slag1	1 g CL
	29	SC8	4 g slag1	4 g CL
SD	30	SD2	1 g slag1	1 g ML
	31	SD8	4 g slag1	4 g ML
ST	32	ST2	1 g slag1	1 g flint
	33	ST8	4 g slag1	4 g flint
S2C	34	S2C2	1 g slag2	1 g CL
	35	S2C8	4 g slag2	4 g CL
S2D	36	S2D2	1 g slag2	1 g ML
	37	S2D8	4 g slag2	4 g ML
S2T	38	S2T2	1 g slag2	1 g ML
	39	S2T8	4 g slag2	4 g ML
BC	40	BC2	1 g BRECEM	1 g CL
	41	BC8	4 g BRECEM	4 g CL
BD	42	BD2	1 g BRECEM	1 g ML
	43	BD8	4 g BRECEM	4 g ML
BT	44	BT2	1 g BRECEM	1 g flint
	45	BT8	4 g BRECEM	4 g flint

Standard patterns from the ICDD Powder Diffraction File [21] were used to provide Miller indices and initial unit cell parameters for all the phases present.

3. Results

An example of the graphical output produced by the pattern fitting procedure is shown in Fig. 1. This example is typical of the quality of fit obtained between observed and calculated data, showing good agreement. This particular mix was found to produce a solid solution phase similar to ettringite. Calcite (main peak at 29.8° 2θ) and dolomite (main peak at 31° 2θ) were also included in the fitting procedure. The enhanced relative intensities of the (1 0 0) and (1 1 0) reflections (9° and 15° 2θ, respectively) for the ettringite phase show that there is a high degree of preferred orientation present.

The refined unit cell parameters produced were inspected for trends with time and mix composition.

The variation with time of the unit cell parameters showed no particular dependence upon the mix compositions. Fig. 2 shows how the unit cell parameters of the thaumasite-like phase produced in mix OC2 varied with time. The unit cell parameters decreased steadily with time and, after 2 years, are close to those of thaumasite. Most of the other mixes that showed a steady change with time (OD2, OD4, OT2, OT8, OSC4, OSD2, OSD4, OSD8, OS2C2, OS2C4, OS2T2, SC8, SD8) also exhibited a decrease in the unit cell dimensions of the thaumasite/ettringite present with time.

A total of eight mixes (OC4, OST4, OS2D2, OS2D4, OS2T4, OS2T8, ST8, BT8) showed no variation of the unit cell parameters with time. A further 16 mixes (OC8, OD8, OT4, OSC2, OSC8, OST2, OST8, OS2C8, OS2D8, S2C8, S2D8, S2T8, BC2, BC8, BD2, BD8) showed an apparently random variation in unit cell parameters with time. In the remaining mixes (SC2, SD2, ST2, S2C2, S2D2, S2T2, BT2), gypsum was the only sulfate mineral produced. No thaumasite/ettringite was detected.

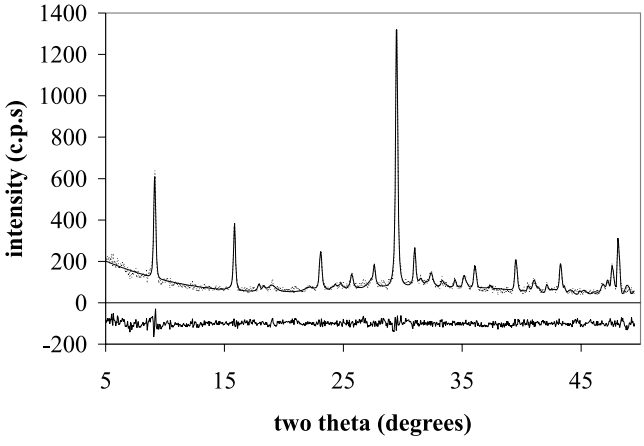

Fig. 1. Comparison of observed and calculated patterns from full pattern fitting. Upper plot: dotted line – observed pattern; solid line – calculated pattern. Lower plot: difference.

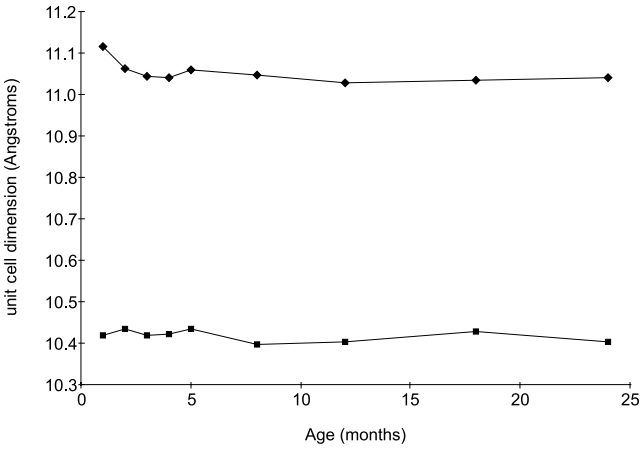

Fig. 2. Unit cell variation with time of mix OC2: diamond – *a*-dimension; circle – *c*-dimension.

In general, there is no significant change in unit dimensions from 18 to 24 months and the reaction products can be considered final.

Table 3 identifies the sulfate minerals produced in each mix at various ages. The initial pH and the pH after two years are also recorded.

OPC slurry mixes containing CL or ML produced significant amounts of thaumasite, or phases similar to thaumasite. The general trend was the initial formation of ettringite and gypsum, followed by a thaumasite-type phase. OPC/flint mixes gave mainly ettringite and gypsum.

In the mixes where the cement component was an OPC/slag mix, those containing flint aggregate performed similarly to the OPC mixes with ettringite and gypsum being the main sulfate minerals. In mixes containing a carbonate aggregate, the results were very different from the equivalent OPC slurries. The only thaumasite phases detected were traces of a thaumasite–ettringite solid solution in two mixes containing ML.

The slurries containing slag with no OPC constituent produced either gypsum or ettringite with no trace of thaumasite. In general, the slurries with the higher water:solid ratio produced gypsum, while the slurries with the lower ratio produced ettringite.

In the slurries containing BRECEM, the sulfate minerals are again limited to ettringite and gypsum with no thaumasite.

Three of the mixes containing ML (OD2, OD4, OSD2) produced two thaumasite/ettringite phases, one

Table 3
Identification of sulfate minerals formed

Mix	Initial pH	pH at 2 yr	Age in months					
			1	2	8	12	18	24
1	12.5	12.5	G, T	T, G	T	T	T	T
2	12.5	12.5	G, T	T, G	T	T	T	T
3	12.5	12.5	E	E	E	E	E	E
4	12.5	12.5	G, E	G, T, E	T, E	T, E	T, E	T, E
5	12.5	12.5	G, E	E, T	E, T	E, T	T, E	T, E
6	12.5	12.5	E	T, E	E	T	E	E
7	12.5	12.5	G, E	G, E	E	E	E	E
8	12.5	12.5	G, E	E, G	E	E	E	E
9	12.5	12.5	E	E, G	E	E	E	E
10	8.5	10.5	G	G	G, E	G, E	G, E	E, G
11	10.5	11.5	E, G	E	E	E	E	E
12	10.5	12.5	E	E	E	E	E	E
13	8.5	10.5	G	G	G	E, G	T, E	T, E
14	10.5	11.5	G, E	G, E	E	E	E	E
15	12	12	E	E	E	E	E	E
16	8.5	10.5	G	G	G,E	E, G	E	E
17	11	11.5	E, G	E	E	E	E	E
18	11.5	12	E	E	E	E	E	E
19	8.5	11	G	G	G, E	E, G	E	E
20	11.5	11.5	E	E	E	E	E	E
21	12	12	E	E	E	E	E	E
22	8	10.5	G	G	E	E	E	E
23	10.5	11.5	E, G	E	E	E	E	E
24	11.5	12.5	E	E	E, G	E, G	E, G	E, G
25	8	10.5	G	G	E	E	E	E
26	11	11.5	E, G	E	E	E	E	E
27	11.5	12	E	E	E	E	E	E
28	8	7.5	–	G	G	G	G	G
29	10.5	11.5	G	E	E	E	E	E
30	8	7.5	–	–	G	G	G	G
31	10.5	12.5	E	E	E	E	E	E
32	8	7.5	–	G	G	G	G	G
33	10.5	11	E	E	E	E	E	E
34	8	9	G	G	G	G	G	G
35	11	10.5	E, G	E	E	E	E	E
36	8	7.5	G	G	G	G	G	G
37	11	11	E	E	E	E	E	E
38	8	9	G	G	G	G	G	G
39	11	11	E	E	E	E	E	E
40	8	9	G	G	E	E	E	E
41	11	11.5	E, G	E, G	E, G	E	E	E
42	8	8.5	–	G	E, G	E	E	E
43	10.5	11	E, G	E, G	E	E	E	E
44	8	9.5	G	G	G	G	G	G
45	10.5	12	E	E	E	E	E	E

E = ettringite-like phase; T = thaumasite-like phase; G = gypsum; – = no sulfate mineral formed.

being similar to ettringite and the other thaumasite-based.

Table 4 shows the unit cell parameters of the thaumasite/ettringite phases present in the mixes at two years. Fig. 3 shows this information graphically as a "unit cell map", with the *c*-dimension plotted against the *a*-dimension. By comparison with unit cell parameters for synthetically prepared solid solutions [10–14], the mixes, for the purposes of discussion, can be separated into several categories (labelled A–F):

A Ettringite-type phases lying close to the ettringite end member. These phases can be considered to be ettringite. This category contains the eight mixes with an a-dimension greater than 11.20 Å. Included in this is the ettringite-type phase formed in two of the three mixes that produced both an ettringite-type and a thaumasite-type phase. Also amongst these eight mixes are four of the mixes containing BRECEM, as well as two of the OPC/flint mixes (OT2, OT4).

Table 4
Unit cell parameters

Series	Mix number	Mix code	Unit cell dimensions (Å)	
			a	*c*
OC	1	OC2	11.042	10.404
	2	OC4	11.084	10.473
	3	OC8	11.122	21.430
OD	4	OD2	11.244	21.269
			11.075	10.470
	5	OD4	11.227	21.424
			11.052	10.503
	6	OD8	11.241	21.400
OT	7	OT2	11.216	21.512
	8	OT4	11.214	21.440
	9	OT8	11.192	21.367
OSC	10	OSC2	11.191	21.308
	11	OSC4	11.194	21.359
	12	OSC8	11.192	21.341
OSD	13	OSD2	11.267	21.394
			11.092	10.539
	14	OSD4	11.170	21.339
	15	OSD8	11.172	21.359
OST	16	OST2	11.185	21.308
	17	OST4	11.185	21.359
	18	OST8	11.200	21.336
OS2C	19	OS2C2	11.174	21.373
	20	OS2C4	11.184	21.382
	21	OS2C8	11.196	21.331
OS2D	22	OS2D2	11.170	21.243
	23	OS2D4	11.185	21.315
	24	OS2D8	11.136	21.338
OS2T	25	OS2T2	11.179	21.272
	26	OS2T4	11.19	21.319
	27	OS2T8	11.198	21.358
SC	28	SC2	No thaumasite/ettringite detected	
	29	SC8	11.194	21.389
SD	30	SD2	No thaumasite/ettringite detected	
	31	SD8	11.163	21.276
ST	32	ST2	No thaumasite/ettringite detected	
	33	ST8	11.218	21.329
S2C	34	S2C2	No thaumasite/ettringite detected	
	35	S2C8	11.193	21.357
S2D	36	S2D2	No thaumasite/ettringite detected	
	37	S2D8	11.187	21.324
S2T	38	S2T2	No thaumasite/ettringite detected	
	39	S2T8	11.183	21.315
BC	40	BC2	11.219	21.402
	41	BC8	11.205	21.446
BD	42	BD2	11.219	21.397
	43	BD8	11.184	21.427
BT	44	BT2	No thaumasite/ettringite detected	
	45	BT8	11.229	21.466

B Phases corresponding to pure thaumasite. This category contains only mix OC2 (1 g OPC + 1 g CL).

C Thaumasite-based thaumasite–ettringite solid solutions. This category contains the thaumasite-type phase present in the mixes that produced both an ettringite-type and a thaumasite-type phase as well as mix OC4.

D Mixes containing a phase corresponding to a sulfate–carbonate ettringite, $Ca_6Al_2(SO_4,CO_3)_3(OH)_{12}\cdot 26H_2O$ [10,12]. Only one mix (OS2D8) falls into this category.

E Mixes which do not correspond to a known solid solution [10–14]. The ettringite-type phase produced alongside a thaumasite-type phase in mix OD2 falls into this category, as well as mixes OC8 and ST8.

F This is the largest category, containing over half of the mixes, including many of those containing slag. The solid solution phases formed in these four mixes

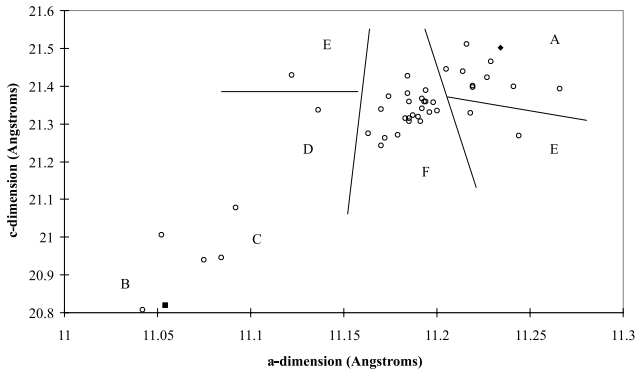

Fig. 3. Unit cell map of thaumasite/ettringite phases after 2 yr: circle – slurry samples; diamond – ettringite; square – thaumasite.

are significantly different from both the thaumasite and ettringite end members of the solid solution, though they are based on the ettringite structure [11]. Some of these mixes correspond to an ettringite–thaumasite solid solution while others can be said to correspond to either the ettringite–thaumasite solid solution or the sulfate–carbonate ettringite solid solution [10–12]. In this region of the figure the two solid solutions cannot be distinguished by unit cell dimensions alone.

4. Discussion

The majority of the mixes studied produced no thaumasite. In general, an ettringite-type phase was produced, varying considerably from "pure" ettringite, as determined by comparison of unit cell parameters. A thaumasite-based product was observed in only five mixes (OC2, OC4, OD2, OD4, OSD2). These five mixes all contained OPC and a carbonate-bearing aggregate at high water:solid ratio (i.e. higher sulfate level). In three of these mixes, the thaumasite was produced alongside an ettringite-like phase.

All but one of the mixes containing slag and all of the mixes containing flint as the aggregate produced no thaumasite. In these mixes, an ettringite-type solid solution was generally produced.

The mixes containing slag and no OPC constituent (numbers 28–39) only produced ettringite/thaumasite at the lower water:solid ratio. At the higher water:solid ratio, gypsum was the only sulfate mineral produced. In the BRECEM mixes (40–45), again only ettringite and gypsum were detected. In four of these mixes, the unit cell parameters show that the ettringite-like phase lies close to the ettringite end member (i.e. in category A in Fig. 3).

The difference observed between the OPC/calcite and OPC/dolomite mixes at high water:solid ratio may be significant. Mixes OC2 and OC4 produced thaumasite only while OD2 and OD4 also produced an ettringite-type solid solution phase. This difference could be due to the different solubilities of the aggregates or to their slightly different carbonate contents, although they only differ by 8 wt%.

Tables 3 and 4 show that the pH and the availability of sulfate have an effect on the identity of the phases produced and on the unit cell of the thaumasite/ettringite present. As mentioned above, in the slag only mixes, the availability of sulfate controls whether gypsum or ettringite is formed. In most other cases, Table 4 shows that the unit cell parameters of the thaumasite/ettringite produced increase with decreasing availability of sulfate. In one case (series OT), the unit cell parameters of the ettringite-type phase produced decrease with decreasing sulfate levels. Decreasing unit cell parameters have been shown to correspond with decreasing sulfate and increasing carbonate [10,12]. In series OC, OD and OSD thaumasite is formed at the higher sulfate levels but not at lower levels.

Work by Gaze [22] suggested that, in her experiment, some gypsum is needed before thaumasite can be formed. Gaze's work showed that the minimum amount of gypsum required is related to the cement's alumina content. There needed to be enough gypsum present to first convert all or most of the alumina into ettringite. Only then can thaumasite form in significant amounts. This may explain why slurries containing slag do not form thaumasite as readily as mixes with just OPC, since slag has a much higher Al_2O_3 content than OPC. A much larger amount of gypsum is therefore required to convert all the alumina in the slag to ettringite, compared to the amount required for OPC. This agrees with the XRD results for slag-containing mixes which all produced large amounts of ettringite-type solid solutions.

5. Conclusions

The results described above show that combining blast furnace slag with OPC stops or possibly retards the formation of thaumasite. OPC mixes produced much thaumasite, but OPC/slag mixes produced only trace amounts and slag-only mixes gave no thaumasite at all.

The work also confirms that formation of thaumasite relies on the presence of a carbonate-bearing aggregate. When flint aggregate is used, no thaumasite was formed.

The exact nature of the ettringite/thaumasite-type phase formed has been found to depend upon the cement and aggregate type, as well as on the amount of sulfate available.

The full pattern fitting technique has proved a valuable tool in this work, highlighting differences between

the thaumasite/ettringite phases formed in the mixes. This is particularly helpful in differentiating the ettringite-type solid solutions formed at different water: solid ratios (and hence different sulfate levels) within each series. Fig. 3 shows that some ettringite-type phases can be identified as either ettringite–thaumasite solid solutions or sulfate–carbonate ettringite solid solutions [10,12] if unit cell parameters are used for identification. In these cases, further investigation would be needed in order to distinguish which of the solid solutions is formed, since at higher Al and/or SO_4^{2-} levels the unit cell parameters of the two solid solutions are quite similar. Accurate measurement of the relative intensities, possible only in the absence of preferred orientation, would enable determination of which solid solution is formed, since the relative intensities of the two solid solutions are very different [10].

Acknowledgements

The authors would like to thank D. Higgins and the Cementitious Slag Makers' Association for their contribution to this work. Part of this work was also funded by the Department of the Environment, Transport and the Regions (DETR).

References

[1] Knill DC. Thaumasite from County Down, Northern Ireland. Mineral Mag 1960;32:416–8.
[2] Hurlbut CS, Baum JL. Ettringite from Franklin, New Jersey. Am Mineral 1960;45:1137–43.
[3] Crammond NJ. Thaumasite in failed cement mortars and renders from exposed brickwork. Cem Concr Res 1985;15:1039–50.
[4] Bensted J. Thaumasite – background and nature in deterioration of cements, mortars and concretes. Cem Concr Compos 1999;21:117–21.
[5] Lachaud R. Thaumasite and ettringite in construction materials. Annales de l'Institut du Batiment et des Travaux Publics 1979;32:370–3.
[6] Report of the Thaumasite Expert Group, The thaumasite form of sulfate attack: risks, diagnosis, remedial works and guidance on new construction. Her Majesty's Stationery Office, London, 1999.
[7] Edge RA, Taylor HFW. Crystal structure of thaumasite. Acta Crystallogr B 1971;27:594–601.
[8] Struble LJ. Synthesis and characterisation of ettringite and related phases. In: Proceedings of the VIIIth International Congress on the Chemistry of Cement, 1987. p. 582–8.
[9] Moore AE, Taylor HFW. Crystal structure of ettringite. Acta Crystallogr B 1970;26:386–93.
[10] Barnett SJ. X-ray Powder diffraction studies of ettringite and related systems. PhD Thesis, Staffordshire University, Stoke-on-Trent, UK, 1998.
[11] Barnett SJ, Adam CD, Jackson ARW. Solid solution between ettringite and thaumasite. J Mater Sci 2000;35(16):4109–14.
[12] Pöllmann H, Kuzel H-J, Wenda R. Solid solutions of ettringites: Part I: Incorporation of hydroxide and carbonate ions in $3CaO \cdot Al_2O_3 \cdot 3CaSO_4 \cdot 32H_2O$. Cem Concr Res 1990;20:941–7.
[13] Pöllmann H, Auer St, Kuzel H-J, Wenda R. Solid solutions of ettringites: Part II: Incorporation of $B(OH)_4^-$ and CrO_4^{2-} in $3CaO \cdot Al_2O_3 \cdot 3CaSO_4 \cdot 32H_2O$. Cem Concr Res 1993;23:422–30.
[14] Buhlert R, Kuzel H-J. The replacement of Al^{3+} by Cr^{3+} and Fe^{3+} in ettringite. Zement-Kalk-Gips 1971;2:83–5.
[15] Kollmann H, Strübel G. Ettringite–thaumasite mixed crystals of brenk (Eifel). Chem Erde 1981;40:110–20.
[16] Langford JI, Loüer D. Powder diffraction. Rep Prog Phys 1996;59:131–234.
[17] Gutteridge WA. Quantitative X-ray powder diffraction in the study of some cementive materials. Proc Br Ceram Soc 1984;35:11–23.
[18] Barnett SJ, Adam CD, Jackson ARW, Hywel-Evans PD. Identification and characterisation of thaumasite by XRPD techniques. Cem Concr Compos 1999;21:123–8.
[19] Halliwell MA, Crammond NJ. Two-year report on avoiding the thaumasite form of sulfate attack. BRE Lab Report, BR385, CRC Ltd., UK, 2000.
[20] Adam CD. IUCr Powder Diffraction Symposium. Toulouse, France, 1990.
[21] ICDD Powder Diffraction File (1989), Card numbers 25-128, 37-1476, 36-1465, 21-816, 36-426, 5-586, 33-1161, 29-285, 4-733.
[22] Gaze ME. The effects of varying gypsum content on thaumasite formation in a cement:lime:sand mortar at 5 °C. Cem Concr Res 1997;27:259–65.